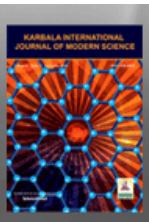

Karbala International Journal of Modern Science

Volume 8 | Issue 2 Article 3

Ultrasound-assisted Dibutyl phthalate nanocapsules preparation and its application as corrosion inhibition coatings

Uday Bagale
Department of food and biotechnology, South Ural State University, Russia, udaybagale@gmail.com

Ammar Kadi
Department of food and biotechnology, South Ural State University, Russia

Irina Potoroko
Department of food and biotechnology, South Ural State University, Russia

Vinay Rangari
Department of civil engineering, Sree Vidyaniketan Engineering College, Tirupati, India

Minakshi Mahale
Faculty of eduction, Bapushaheb D D Vispute, Dhule, India

Ultrasound-assisted Dibutyl phthalate nanocapsules preparation and its application as corrosion inhibition coatings

Abstract

The current research employs an encapsulation of dibutyl phthalate (DBP) as a corrosion inhibitor in situ polymerization using a sonochemical method to form nanocapsules. The prepared nanocapsules were characterization by using Malvern particle size, Fouri-er transforms infrared spectroscopy (FTIR), Scanning electron microscope (SEM) and Transmission electron microscope (TEM), and thermal and mechanical test to check particle size, morphology, and stability of nanocapsules. Later prepared DBP nanocapsules were incorporated in standard epoxy coating to check its corrosion inhibition resistance. The results show that nanocapsules are spherical, with an average particle size of 337 nm. Scratch nanocapsules epoxy coating shows improves coating resistance after 1 day immersion, the values shown for 10% nanocapsules-based coating 8.62 x 1010 while for scratch standard coating is 2.41 x103. Overall thermal and mechanical properties for nanocapsules show better resistance, and electrochemical characterization for scratch nanocapsules coating shows better results than scratch epoxy coating

Keywords

Dibutyl phthalate; In-situ polymerization; ultrasound-assisted; Corrosion inhibition coating; and Electrochemical analysis

RESEARCH PAPER

Ultrasound-Assisted Dibutyl Phthalate Nanocapsules Preparation and its Application as Corrosion Inhibition Coatings

Uday Bagale [a,*], Ammar Kadi [a], Irina Potoroko [a], Vinay Rangari [b], Minakshi Mahale [c]

[a] Department of Food and Biotechnology, South Ural State University, Russia
[b] Department of Civil Engineering, Sree Vidyaniketan Engineering College, Tirupati, India
[c] Faculty of Eduction, Bapushaheb D D Vispute, Dhule, India

Abstract

The current research employs an encapsulation of dibutyl phthalate (DBP) as a corrosion inhibitor in situ polymerization using a sonochemical method to form nanocapsules. The prepared nanocapsules were characterization by using Malvern particle size, Fourier transforms infrared spectroscopy (FTIR), Scanning electron microscope (SEM) and Transmission electron microscope (TEM), and thermal and mechanical test to check particle size, morphology, and stability of nanocapsules. Later prepared DBP nanocapsules were incorporated in standard epoxy coating to check its corrosion inhibition resistance. The results show that nanocapsules are spherical, with an average particle size of 337 nm. Scratch nanocapsules epoxy coating shows improves coating resistance after 1 day immersion, the values shown for 10% nanocapsules-based coating 8.62×10^{10} while for scratch standard coating is 2.41×10^{3}. Overall thermal and mechanical properties for nanocapsules show better resistance, and electrochemical characterization for scratch nanocapsules coating shows better results than scratch epoxy coating.

Keywords: Dibutyl phthalate, In-situ polymerization, Ultrasound-assisted, Corrosion inhibition coating, Electrochemical analysis

1. Introduction

Problem-related corrosion occurs in every part of the industry, mainly in the oil, pipe, and automotive sectors, with repairing corrosion costs across $2.5 trillion [1,2]. The cost of corrosion repairing in India crossed 4−5% of total GDP, equivalent to $70 billion [2,3]. Organic coating develops aesthetic appearance and protective properties to minimize the problem caused by corrosion [3−8]. The researcher concentrated on developing a corrosion inhibitor blend polymer as a protective coating. Furthermore, they developed a polymer or composite which shows barrier properties against environmental oxygen or moisture and self-repairing properties [9−12]. However, such coatings have limitations, so, currently, the microencapsulation technique was used to create an innovative polymeric material for corrosion inhibition [12−14]. Microencapsulation can be accomplished with various techniques, including interfacial polymerization, coacervation/phase separation, solvent evaporation, suspension cross-linking, emulsion polymerization, and others, such as the layer-by-layer (LBL) method [10,11,15]. Self-healing polymeric materials using microcapsules/nanocapsules are a prime example of such a technique [3,12,13,16]. These innovative polymeric coatings, such as microvascular and molecular epoxy-based smart coatings containing compartmentalized solid healing agents, were primarily aimed at the recovery of the mechanical properties of the damaged polymer for a short period [9,10]. Despite these flaws in the current system, the simple design and ease of

Received 10 September 2021; revised 19 February 2022; accepted 23 February 2022.
Available online 1 May 2022

* Corresponding author at: Chelyabinsk 454080, Russia.
E-mail address: udaybagale@gmail.com (U. Bagale).

https://doi.org/10.33640/2405-609X.3218

fabrication materials may make them suitable for developing a new application, such as coatings and elastomer self-healing material [3,9,13,16]. According to the available literature, smart coatings design is desirable for long-term and efficient corrosion protection. However, the majority of the research was conducted in laboratories, often using expensive or toxic chemicals, and was primarily concerned with self-healing chemistry [9–11] and DCPD, epoxy resin, edible oil, core–shell healing agent [17–20].

It was also reported that ceramic or oxide-based nanocontainers were used in the sol–gel coating because of their excellent strong bonding with the host matrix [21–27]. In the case of marine applications, the coating thickness should be greater than 20 μm. A nanosize capsule was recommended for the low film thickness coating to solve the problem. Nanocapsules base coating improves wet adhesion, corrosion resistance, and healing performance [28–34]. For the preparation of nanocapsules, most researchers now use the ultrasound approach technique. The ultrasound phenomenon is characterized by the formation and dissolution of vapor cavities in aqueous media. The acoustic field is created by ultrasonic waves passing through the medium, resulting in a fine dispersion of the two immiscible liquids. The fine dispersion of two phases creates too much-localized turbulence, shattering primary droplets into nanoscale size [35–38].

In this direction, we worked on the nanosize capsules and their preparation for solvent-free self-healing coating. The ultrasound-assisted encapsulation techniques were used to incorporate the epoxy coating for marine application. In some ways, the approach to resolving corrosion issues was synthesizing nanocapsules using ultrasound, catalyst-free intelligent species (dibutyl phthalate (DBP) as plasticizer) in the urea-formaldehyde shell. This approach newer tried by research to date. DBP and ethanol create the ideal conditions for intelligent corrosion inhibition thermosetting matrix. When the coating ruptures, the polymeric urea-formaldehyde shell, which already softens with DBP as a plasticizer, releases the core DBP with ethanol. These core materials soften the epoxy-amine by wetting and swelling the bulk polymer. When the ethanol in the coating evaporates, the crack coating forms another layer of epoxy-amine polymerized film. Because dibutyl phthalate has a higher molecular weight, it has less volatility and permeability through the shell wall, resulting in capsules with more excellent stability [39–43]. Electrochemically active compounds cause corrosion inhibition in the DBP, such as fatty acid, phenolic, and ketones groups.

Further, it also contains oxygen with aromatic compounds in a backbone structure with corrosion inhibition properties. By using in-situ emulsion polymerization, these aspects, dibutyl phthalate and ethanol were encapsulated in a urea-formaldehyde shell. Nanocapsules were prepared and added to a coating formulation for electrochemical analysis using Bode and Nyquist plots.

2. Material and methods

2.1. Materials

Formaldehyde, ammonia chloride, urea, polyvinyl alcohol, and resorcinol were purchased from M/s Alfa-Aesar, India. Industrial epoxy resin (Epoxy equivalent weight 187 g/eq, 70% solid content), hardener (60% solid content and Viscosity 2000 cP), and reactive diluents (Epotec RD 108) were obtained from M/s Pidilite Ltd (India), whereas; Sorbitan monooleate (Span 80), Dibutyl phthalate (LR Grade) was obtained from Sigma–Aldrich. DM water was used during all the experimentations.

2.2. Preparation methods of nanocapsules

2.2.1. Preparation of prepolymer urea-formaldehyde solution

2.5 g of urea was liquefied in 5 g of 37% formalin. Then pH of the solution was adjusted 8 by the addition of triethanolamine. Then Dakshin Ultrasound (20 kHz with a power of 140 W) mixture sonicated for 20 min at room temperature. Furthermore, 20 ml water was added to the solution to form a prepolymer urea-formaldehyde solution.

2.2.2. Nanocapsules fabrication

As reported in our previous work, Uday et al. [38], a modified procedure for fabrication of nanocapsules as follows: for preparation of surfactant solution, we took span 80 dissolves in 20 ml of water and then added in prepared 5% PVA solution (30 ml). Further Prepolymer UF solution was added to this surfactant solution and sonicated for 5 min. After some time, a 5 ml of dibutyl phthalate solution in 10 ml ethanol was gently added for encapsulation in emulsion and sonicated 20 min until homogeneous stabilization occurs. Later sonication was stopped, and the pH was accustomed to 3.5 with acid addition. After pH adjustment, the emulsion was stirred and sonicated for 40 min at 50 °C still the reaction stage was completed. The nanocapsules were filtered and cleaned when the emulsion had

cooled to room temperature. These nanocapsules were dried overnight at 45 °C and stored in the airtight container for future usage.

2.3. Characterization of nanocapsules

A Field emission scanning electron microscope (FESEM) and a transmission electron microscope (TEM) were used to investigate the structural morphology of nanocapsules. A particle size analyzer was utilized to understand the size distribution of nanocapsules. The Fourier transform An infrared spectrophotometer with a wavelength range of 4000-400 cm^{-1} was used to identify the functional group contained in nanocapsules. A differential scanning calorimeter was used to test the thermal stability of nanocapsules throughout a temperature range of 30–350 °C. Stress generation or capsule rupture were used to test the stability of nanocapsules concerning agitation time, speed, and different viscosity epoxy resin solutions.

2.3.1. Surface preparation and coating formulation and their corrosion performance on mild steel surfaces

To ensure a better bond among the coating and substrate, the mild steel surface was dipped in soap solution to remove any lubricant oil and dirt present on the panel surface. This treated surface also contributes to the final coating's aesthetic properties. To create a corrosion-inhibiting coating, nanocapsules were added to an epoxy solution along with wetting and dispersant additives. The polymer to hardener ratio was kept constant at 4:1. The amine hardener was mixed into the nanocapsules epoxy homogeneous solution before applying it to the steel surface. Nanocapsules in three concentrations, 2.5, 5, and 10%, is added to the coating formulation. The coating was applied to the mild steel surface using a brush and allowed to dry for 3–4 days before the analysis. The dry thickness was observed to be average 120 ± 5 μm. Electrochemical measurements of corrosion inhibition performance for Bode and Nyquist plots were performed on scratch-coated panels with and without nanocapsules. Coated panels were immersed in 3.5% salt solution for 14 days for the Bode and Nyquist plot, and the impendence was measured in the uniform time interval (or 1 day and 14 days immersion) with the frequency of 10^{5}– 10^{-2} Hz.

3. Results

The present study used sonicated in-situ emulsion polymerization to create dibutyl phthalate (DBT) nanocapsules with a polymeric shell of urea and formaldehyde. A liquid core was enclosed within this polymeric shell, generated under acidic circumstances. Polymerization was carried out with urea and formaldehyde, with the reaction mass's molecular weight increasing as polymerization progressed. The urea-formaldehyde polymer had a hydrophilic bulk at the end of the polymerization reaction. This polymer is recovered from an aqueous phase adsorbed on the hydrophobic phase, forming a thick polymeric shell on the emulsified core. Fig. 1 shows fabrication and the schematic DBP nanocapsules for corrosion inhibition.

3.1. Morphology and size analysis of nanocapsules

We examine the capsule encapsulation stability, size, and aggregation in an epoxy matrix and morphology of shell material thickness using FESEM and TEM images. Initially, dried gold sputter nanocapsules samples were prepared on glass slides for FESEM measurements at 5.0 kV. The morphology of nanocapsules with a monodisperse size distribution is depicted in Fig. 2. Nanocapsules were discovered to be spherical, with thick polymeric shells and corrosion inhibitors encapsulated (as demonstrated in TEM and FESEM image). As shown in Fig. 2, the capsule has two layers: one for the shell and one for the smooth inner layer where dibutyl was protected as the core. Using image j software for FESEM image, the average thickness of the surface inner wall is 250–270 nm, while the thickness of the outer surface is 80–100 nm. With the optimized surfactant concentration, FESEM investigated clumping problems caused by low surfactant concentration, and less aggregation was observed in the FESEM and TEM (average particle size in range 330–350 nm) as shown in Fig. 2. Capsules were processed using the optimized capsule preparation process and were dispersible in epoxy, as shown in Fig. 3. The visual image of stable capsules revealed the same behavior as the stability of nanocapsules in the dispersion phase. The average capsule size was 337 nm, and the polymer dispersity index was 0.47. Our previously published article shows that increasing the sonication time can reduce particle size compared to the conventional agitation method [38].

3.2. FTIR analysis of nanocapsules

Figure 4 depicts an FTIR analysis of UF resin and nanocapsules. It was discovered that the majority of the amide group was identified at 2925 cm^{-1}, C=O bond at 2353 cm^{-1}, C–H bending at 1463 cm^{-1}, C–N stretching at 1275 cm^{-1}, C–O stretching at

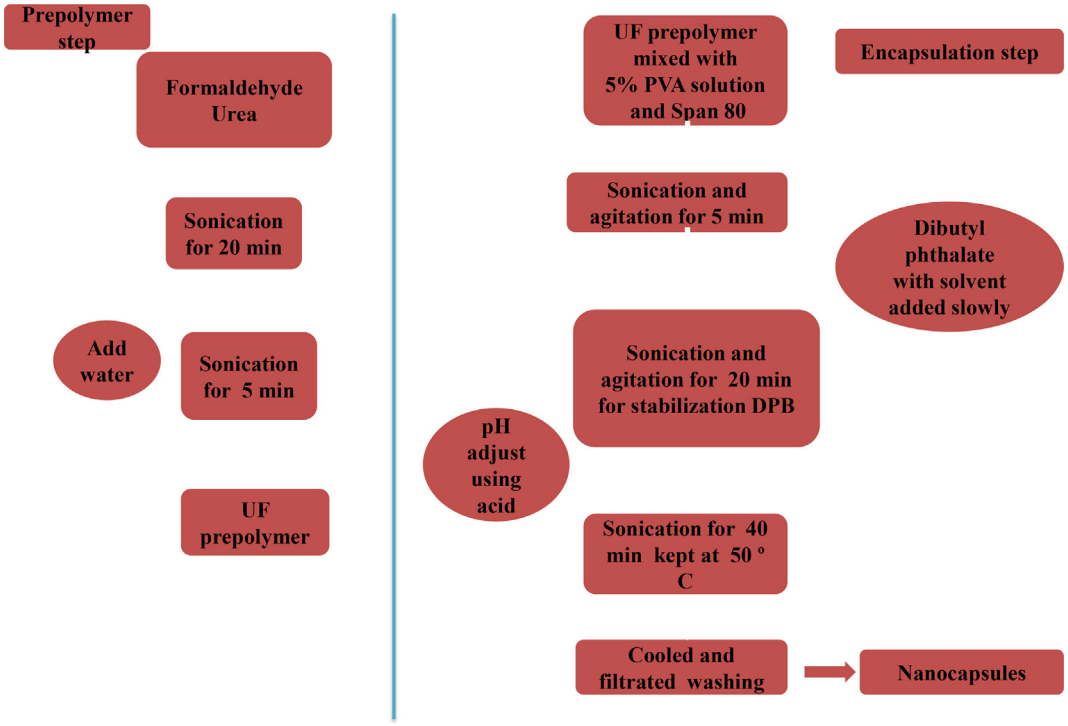

Fig. 1. Graphic demonstration of the technique for production of nanocapsules.

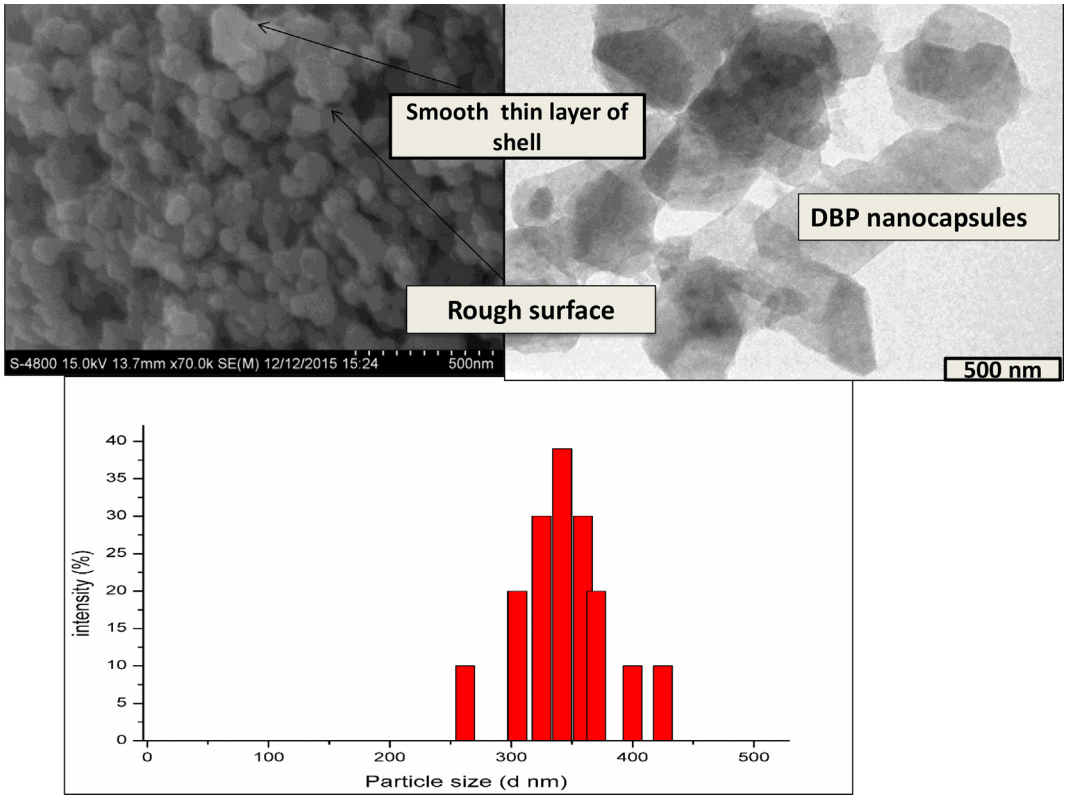

Fig. 2. FESEM, TEM, and Particle size analysis of nanocapsules based on DBP (Dibutyl phthalate).

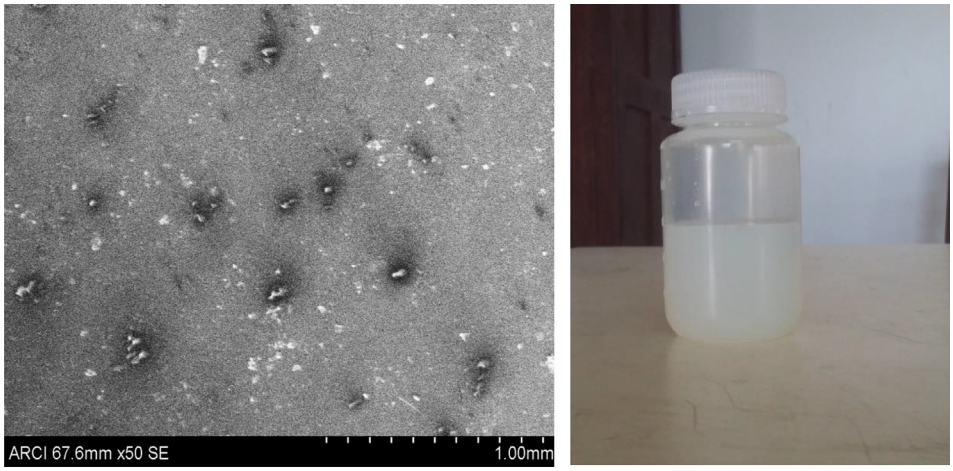

Fig. 3. SEM image of nanocapsules (DBP) dispersed in the epoxy-amine coating.

1193 $cm^{-1,}$ and C=C bending from 975 to 751 cm^{-1}. The characteristic peaks indicate that dibutyl phthalate has been encapsulated in a polymeric shell composed of urea-formaldehyde.

3.3. Thermal analysis of nanocapsules

Figure 5 shows the results of a DSC analysis to determine the thermal stability of nanocapsules in the range of 30–600 °C with a heating rate of 10 °C/min. Fig. 5 shows two endothermic and one exothermic peak for UF resin, as well as an exothermic peak for nanocapsules. Water loss is observed at 100 °C, sales, while the second peak is observed at 150–300 °C, corresponding to polymeric shell degradation. The endothermic peaks represent the melting of the polymeric shell. Whereas for nanocapsules, the elevation decreases between 200 and 300 °C, indicating that dibutyl phthalate melts between 200 and 270 °C and loses its contents at 200 °C as reported by Jackson et al. [39] (Fig. 5). This test demonstrates that the thermal stability of dibutyl phthalate-based nanocapsules is superior to that of the previously reported healing agent [38].

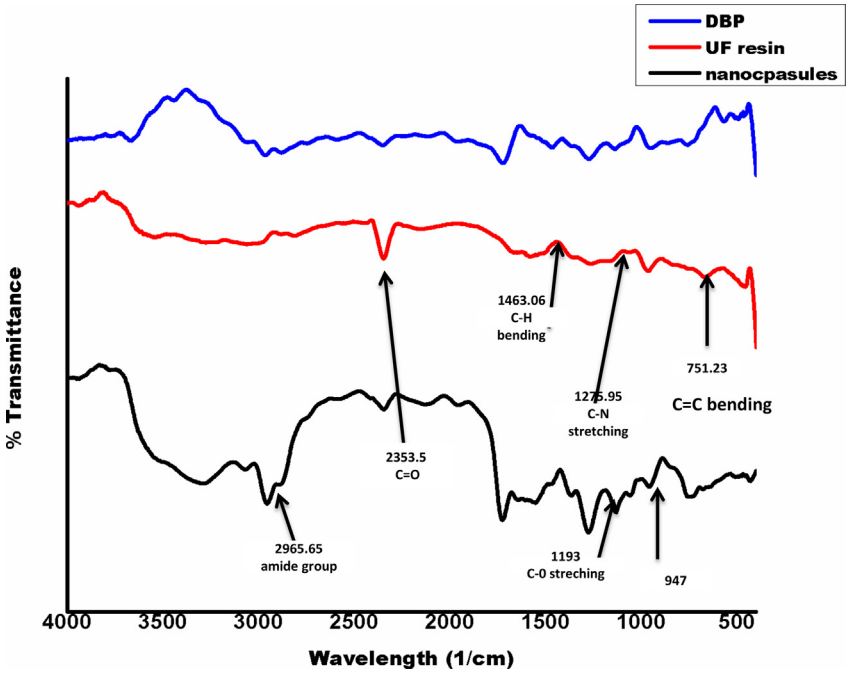

Fig. 4. FTIR spectra analysis for a) DBP, b) UF resin, and c) DBP Nanocapsules.

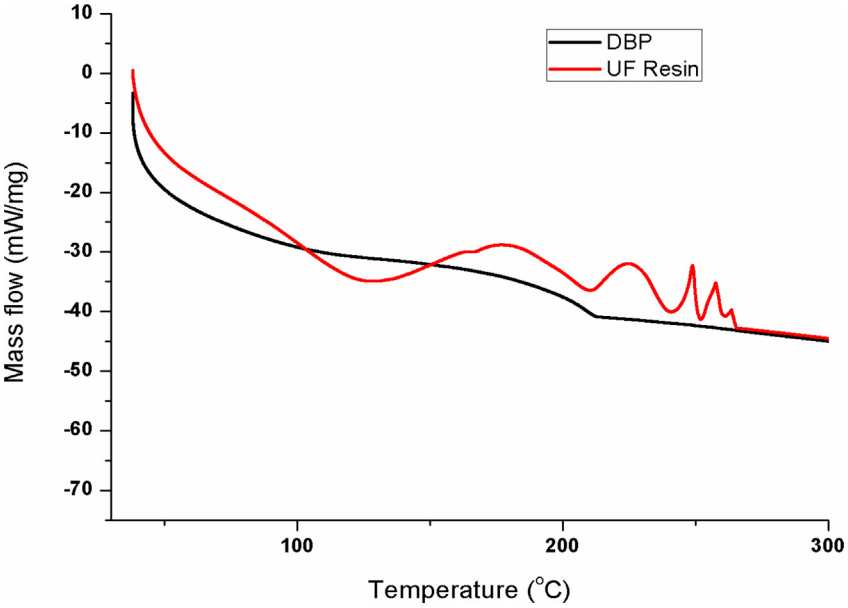

Fig. 5. DSC analysis for DBP nanocapsules and UF resin.

The thermo-gravity analysis of nanocapsules and urea-formaldehyde is shown in Fig. 6. It was discovered that up to 100 °C, both cases have a 2.91% loss of water molecules. Later, as the temperature rises to 200 °C, the nanocapsules have a slight mass loss. At 300 °C, a large portion of the urea-formaldehyde weight loss occurred, i.e., nearly 86.20% weight loss. At the same time, DBP nanocapsules lose slightly less weight (around 21%) at the same temperature. Weight loss is observed to be less as the temperature rises to 450 °C when compared to the UF shell. This occurred due to dibutyl phthalate (DBP) adhering to the surface of urea-formaldehyde, which softens the nanocapsules. Finally, the residual mass of DBP nanocapsules is higher when compared to the UF shell

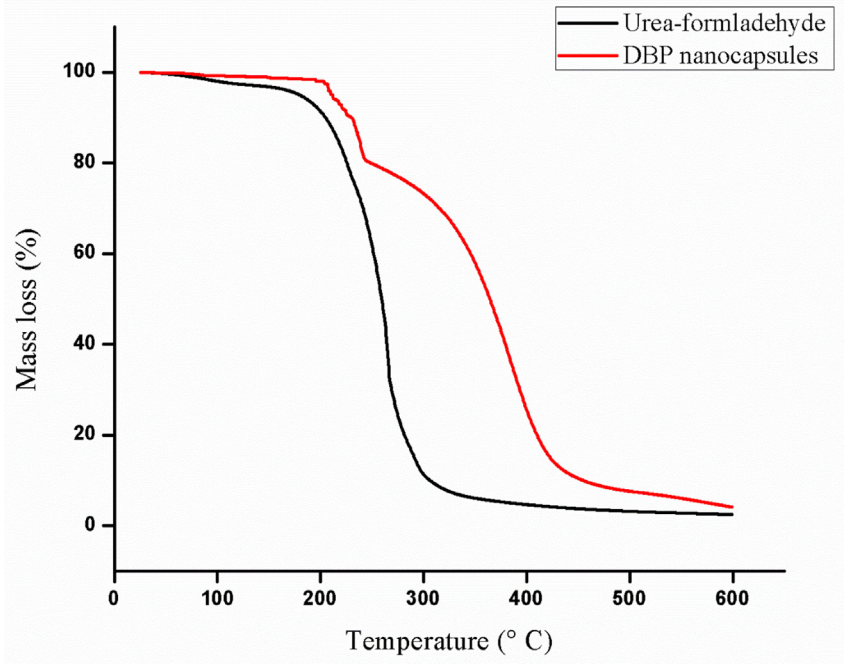

Fig. 6. Thermogravimetric analysis (TGA) of nanocapsules and Urea-formaldehyde.

material. This demonstrates that the DBP nanocapsules have good thermal properties.

3.4. Mechanical stability of nanocapsules

Figure 7a–7(c) shows the mechanical stability of nanocapsules as a function of agitation speed, time, and epoxy solution viscosity. Agitation caused much shear stress during nanocapsules dispersion in coating preparation. As a result, nanocapsules must have a high mechanical strength to withstand stress to remain intact. During the dispersion and application of paint, these nanocapsules should not break. It is predicted that capsules get ruptured if the covering film is damaged at that time, enabling healing material to escape. Three critical parameters, I determine mechanical stability) the viscosity of the paint, ii) the agitator speed (rpm), and iii) the agitation time. Unbroken nanocapsules are observed at a speed of 200 rpm on the agitator. The rupture of nanocapsules increases as the agitation speed increases. It shows that when the agitation speed is near 500 rpm, 70–75% of the nanocapsules rupture. The mechanical stability of nanocapsules is

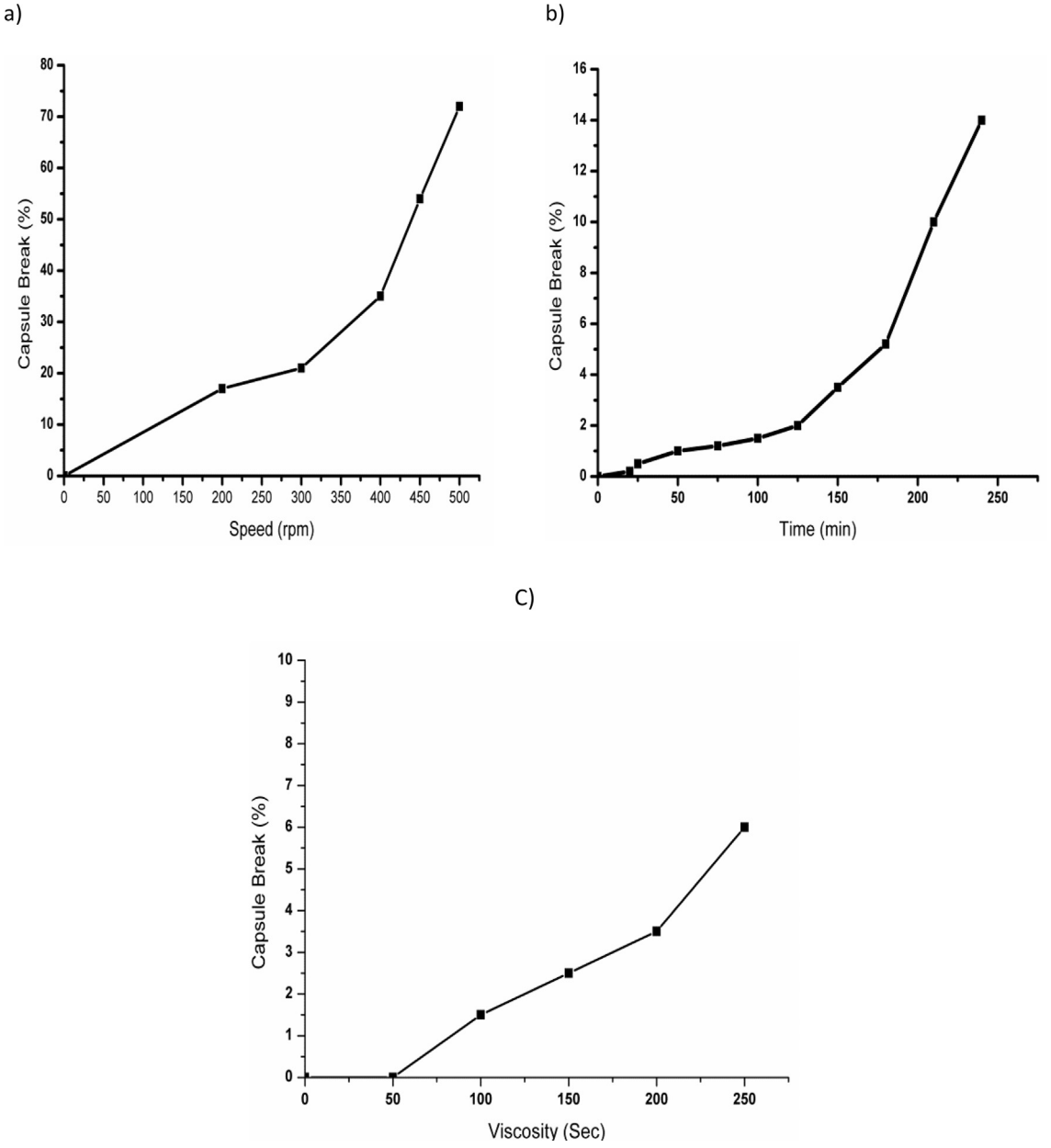

Fig. 7. Mechanical stability of nanocapsules concerning a) agitation speed, b) Time and c) Viscosity.

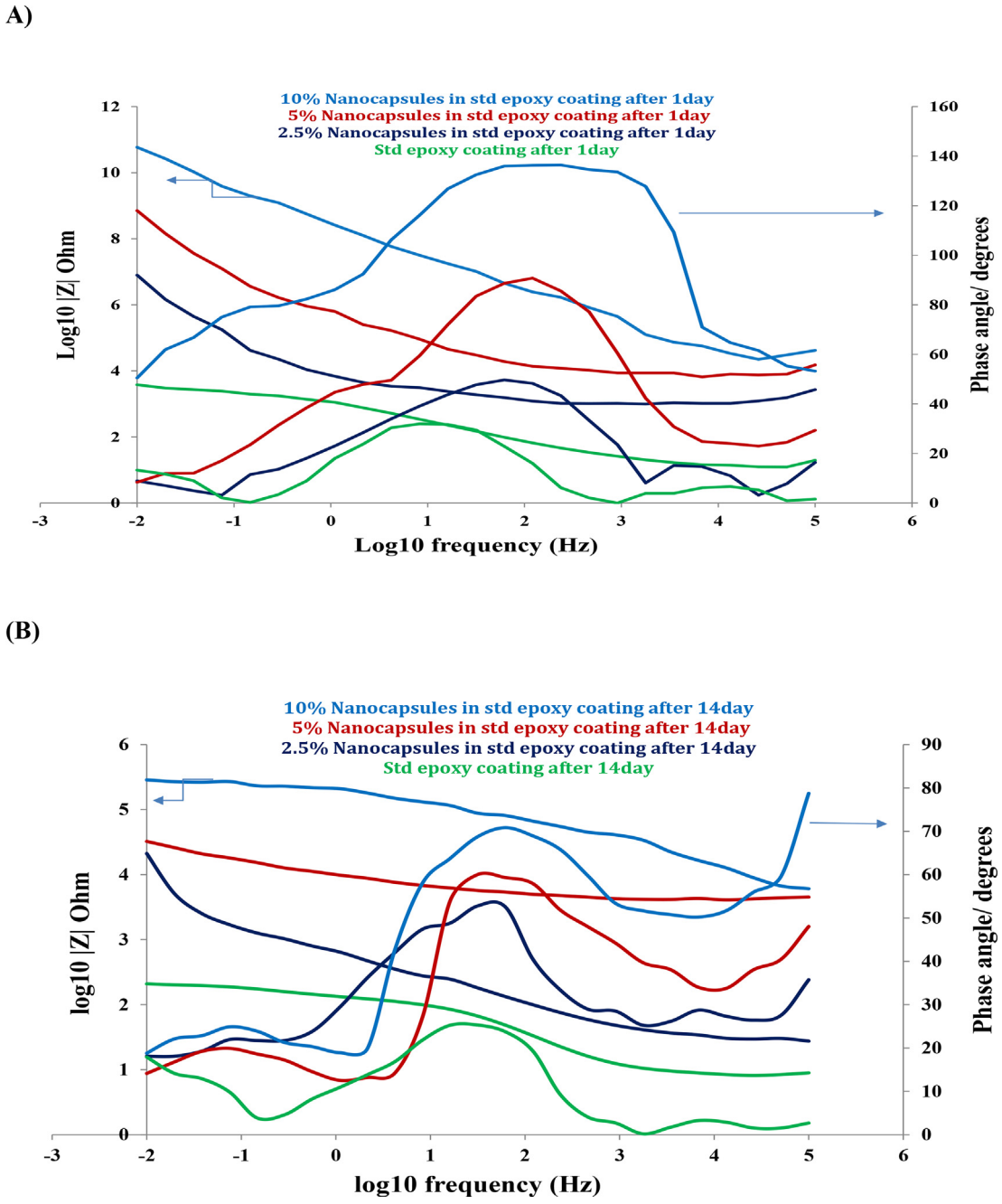

Fig. 8. A–B: Bode plot for the EIS data for samples immersed in 3.5 wt % NaCl aqueous solution A) After 24 h B) After 14 days.

Table 1. EIS parameter data in terms of coating resistance and coating capacitance.

Name of system	Period day of immersion	Coating capacitance (C_c)	Coating resistance (R_c)
Scratch Std epoxy amine coating	1 day	5×10^{-5}	2.41×10^{3}
	14 days	3.8×10^{-5}	7.54×10^{1}
2.5% nanocapsules in Std epoxy coating	1 day	1.94×10^{-6}	4.72×10^{6}
	14 days	5.95×10^{-6}	1.52×10^{4}
5% nanocapsules in Std epoxy coating	1 day	1.90×10^{-8}	4.33×10^{8}
	14 days	2.5×10^{-7}	1.93×10^{4}
10% nanocapsules in Std epoxy coating	1 day	2.4×10^{-10}	8.62×10^{10}
	14 days	1.7×10^{-10}	2.1×10^{5}

affected by continuous agitation. Fig. 7c shows continue agitation has no effect on mechanical stress on nanocapsules (100 min).

Furthermore, this continuous agitation for 4 h results in only 15–20% ruptures of nanocapsules at a speed of 200 rpm. However, when nanocapsules were dispersed in paint formulation at the agitation of around 200 rpm for 30 min, uniform distribution was observed with no rupture of nanocapsules. However, as the viscosity of the solution increased, high shear stress had a substantial influence on the solidity of the nanocapsules. It finds that at a solution viscosity of 250 s, only 6% of the nanocapsules found ruptured. The images of the coating were

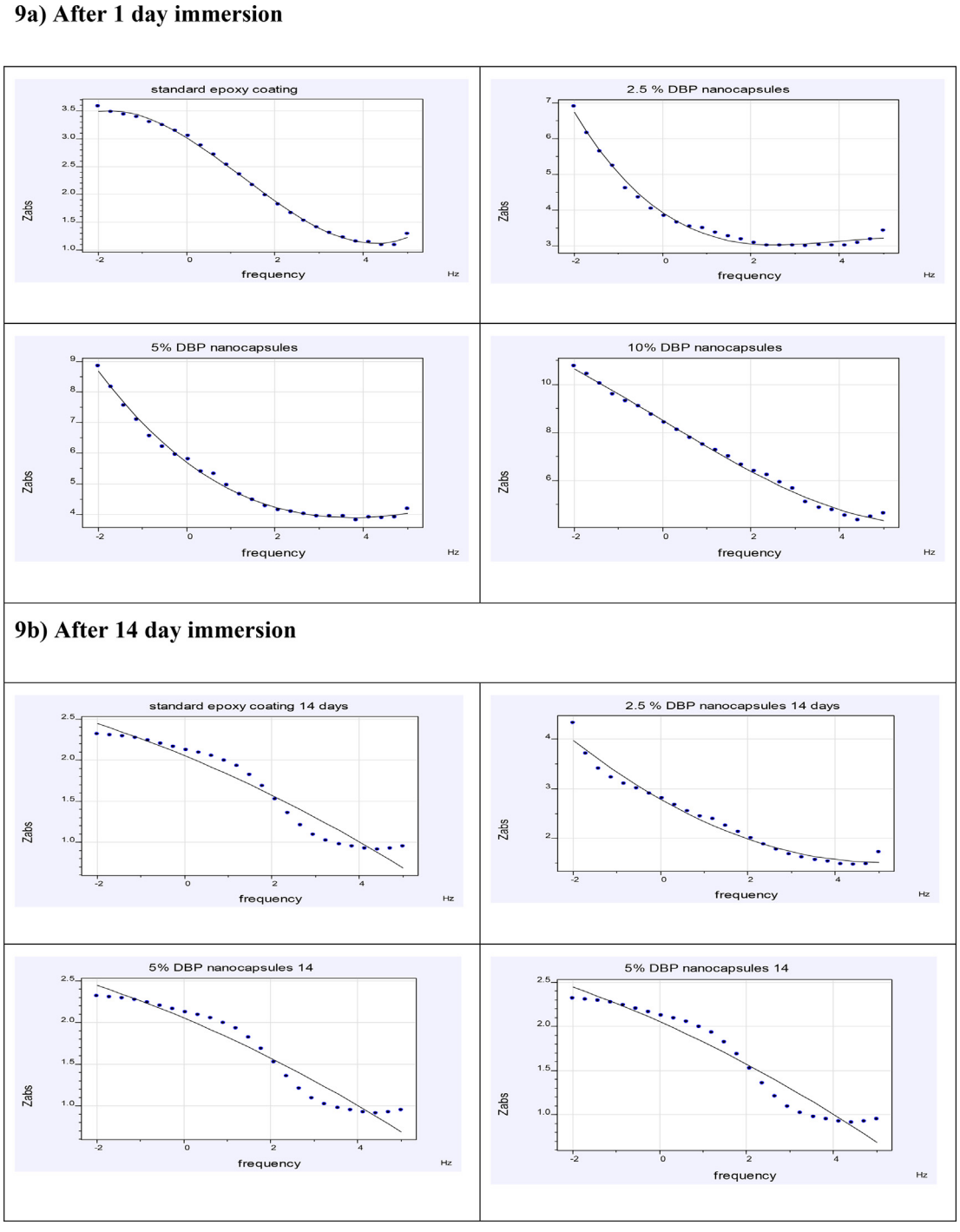

Fig. 9. Curve fitting Bode plot a) After 1st b) After 14th days.

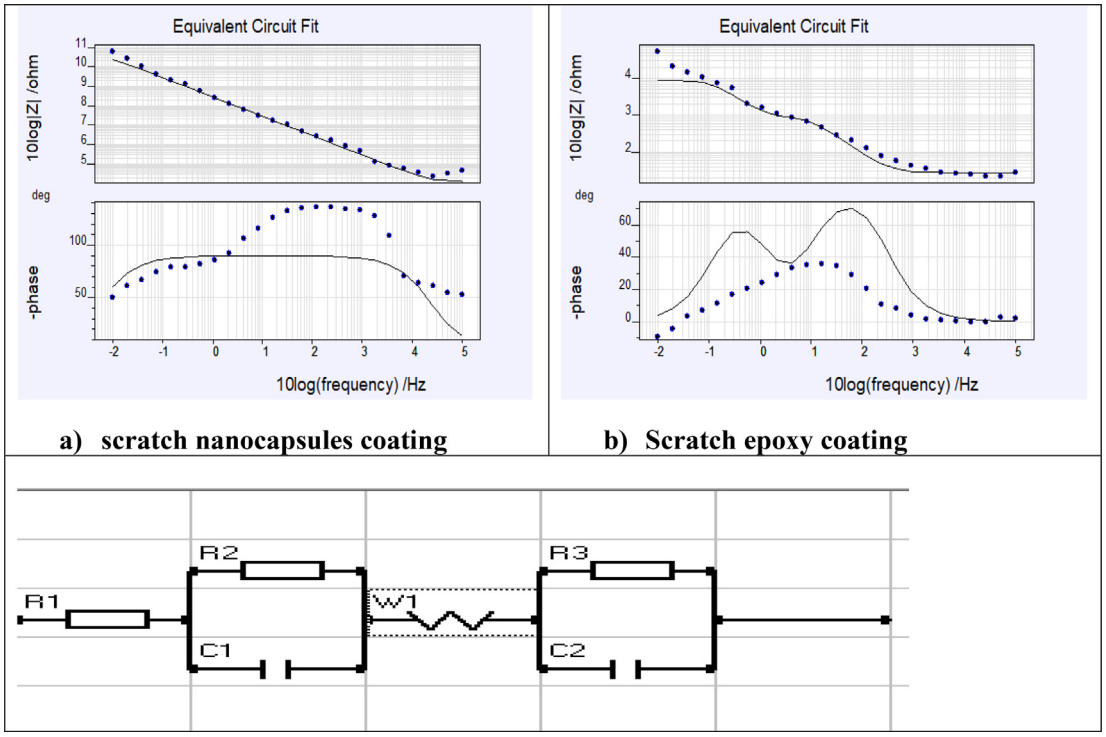

Fig. 10. Equivalent circuit fit impedance data for Bode plot a) Scratch nanocapsules and b) Scratch epoxy coating.

captured using optical microscopy. Compared to previously reported literature, it demonstrates that 70–75% of capsules were ruptured [28].

3.5. Nanocapsules coating electrochemical characterization

Corrosion on surface coating happens due to moisture in the environment and oxygen, causing film rupture. It may be possible to repair the rupture film using a nanocapsule-based coating. To understand the effect of nanocapsules on corrosion inhibitors, we performed an electrochemical analysis. For EIS measurement, Scratch coated Panels (120 μm dry thickness) were kept in a salt solution for 1 and 14 days' time intervals [44–47]. All EIS measurements for scratch epoxy coating and different DBP nanocapsules coating were executed in triplicate. EIS results were formfitting to circuit model using Ivium soft with chi-square value decrease to 10^{-4} or less than to achieve. The chi-square value for standard epoxy coating is 2.16×10^{-1}. The typical six short frequency measurements in the plateau area were used to create the coating resistance layer acquired from the Bode plot. This parameter responds to the existence of ions captivated by the coating film from the nearby environs, indicating the presence of a protective coating. The layer has a higher impendence value than the conducive substance since all polymeric coatings are non-conductive. This coating also creates a barrier between the coating surface and the electrolyte, which helps to prevent corrosion. A high-performance layer with exceptional barrier qualities serves as an almost perfect capacitor when exposed to an electrolyte for the first time. At this point, coating resistance is exceedingly high.

Figure 8A and 8B depict the Bode plot in terms of impendence versus frequency. This figure shows that initially, scratch epoxy after 1 day immersion provided higher resistance log |Z| = 3.7 than 14 days immersion log |Z| = 2.3 as coating get swelling due to adsorption ions through the surface and start the corrosion process. Furthermore, after 1 day and 14 days of immersion (Value for DBP nanocapsules), Scratch DBP nanocapsules epoxy coating outperforms scratch epoxy coating. This is due to dibutyl phthalate, which acts as a self-healing agent, plasticizes the capsules, and prevents any nearby ions from adsorbing onto the surface. After 14 days of immersion, the OCP value of scratch epoxy decreased from −0.437 to −0.57, while the value of DBP nanocapsules decreased from −0.160 to −0.285. To ensure that the data in Table 1 is the same, graphs in terms of coating resistance (Rc) and coating capacitance were made. The initial coating

I) After 1 day immersion

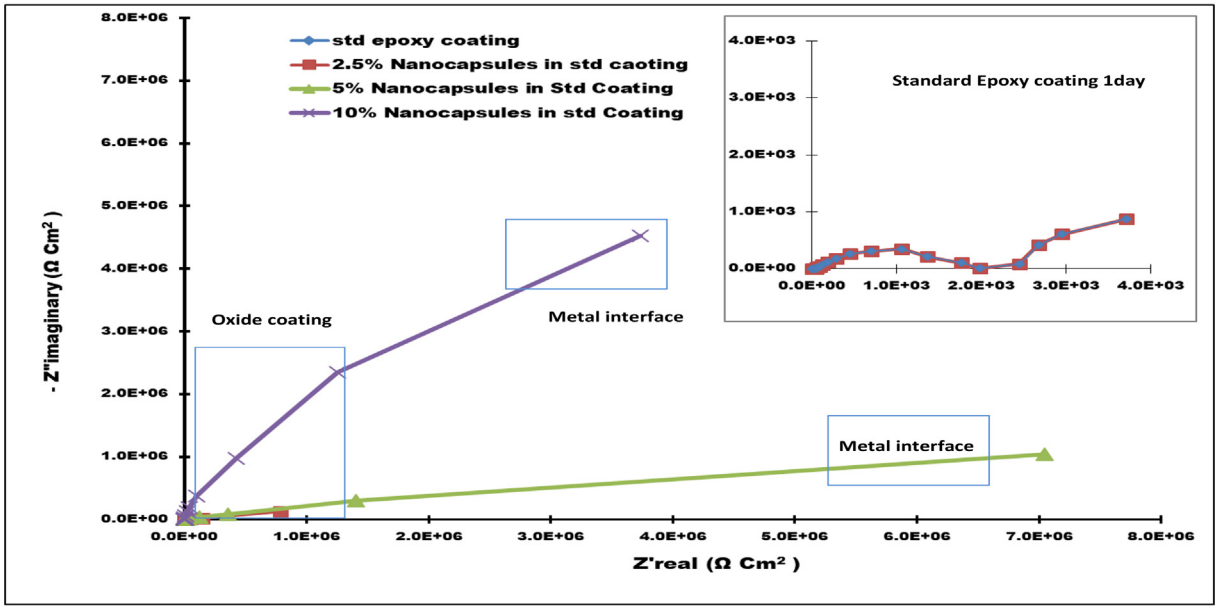

II) After 14 days immersion

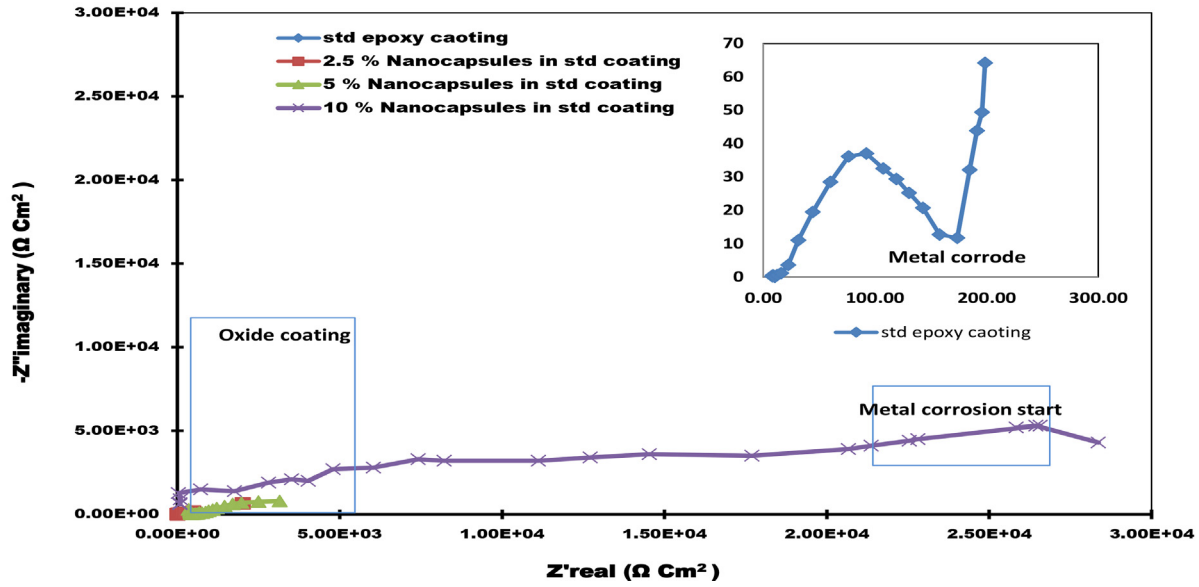

Fig. 11. Nyquist plot for corrosion inhibition nanocomposite coating based DBP I) after 1 day immersion and II) after 14 day immersion.

resistance (R_c) value for nanocapsules coating is 4.72×10^6 cm^2, but as immersion time increases, R_c increases slightly to 7.54×10^1 cm^2. However, in the absence of nanocapsules scratch coating, the coating resistance value after 14 days immersion is more significant than after 1 day immersion for scratch epoxy coating. The results show that the coating resistance value gradually decreases while maintaining a high level of corrosion inhibition performance.

Again, the addition of such nanocapsules improves coating resistance and provides a strong barrier between moisture and the coating substrate. After 1 day immersion, the values shown in Table 1 for nanocapsules-based coating with different concentrations (2.5, 5, and 10%) are 4.72×10^6,

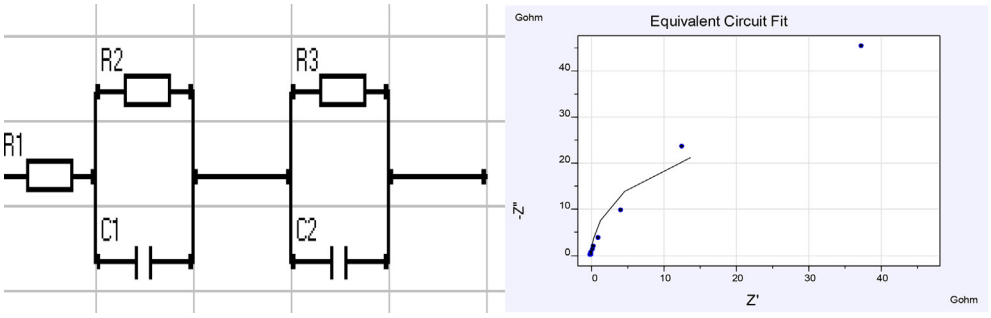

Fig. 12. Suggest equivalent circuit diagram for coating along with equivalent circuit fitting.

Table 2. Fitting parameter of the suitable coating obtained from EIS studies.

	Par Fixed	Value	Error%	Min	Max	Unit
Par 1	R_1	1.160 E^{+04}	1.44	1.0E^{-4}	1.0 E^{+13}	Ohm
Par 2	R_2	4.839 E^{+10}	02.23	1.0E^{-4}	1.0 E^{+13}	Ohm
Par 3	R_3	4.089 E^{+02}	0.100	1.0E^{-4}	1.0 E^{+13}	Ohm
Par 4	C_1	5.786E^{-10}	12.79	1.0E^{-13}	1.0 E^{+1}	F
Par 5	C_2	5.836E^{-08}	10.00	1.0E^{-13}	1.0 E^{+1}	F

4.33×10^8, and 8.62×10^{10}, respectively. After 14 days of immersion, these values were reduced to 1.52×10^4, 1.93×10^4, and 2.1×10^5 for 2.5, 5, and 10% nanocapsules. According to the current findings, we have superior impedance for nanocapsules than standard coating.

Two-phase maxima were observed in Fig. 8A-B phase angle, the major one at lower frequencies corresponding to the protective layer and the other as a shoulder at intermediate frequencies corresponding to the electric double layer. The phase angle values range from 120 to 60°, indicating that the coating acts as a protective agent. This behavior suggests that the coating has improved barrier properties and functions as an insulator. Compared to nanocapsules-based coating, the scratch epoxy amine coating has a phase angle of 10°. The phase angle is between 130 and 60°. After 14 days of exposure in a corrosive environment, the impedance values of nanocapsules-based coating show the best corrosion inhibition in the low-frequency range.

The Curve fitting for individual bode plot of scratch epoxy coating and DBP nanocapsules coating after 1 and 14 day immersion as shown in fig. 9a and b, respectively (IviumSoft show individual curve fitting). Fig. 10 show equivalent circuit fit impedance data for Bode plot a) Scratch nanocapsules and b) Scratch epoxy coating.

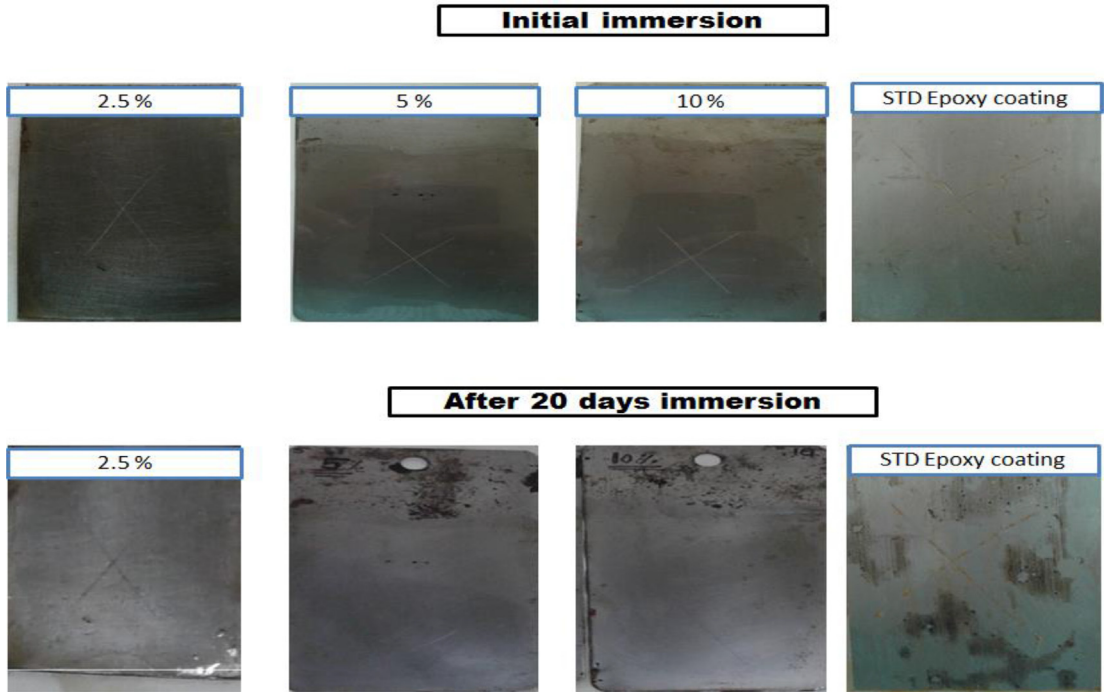

Fig. 13. Immersion test for corrosion inhibition coating based nanocapsules.

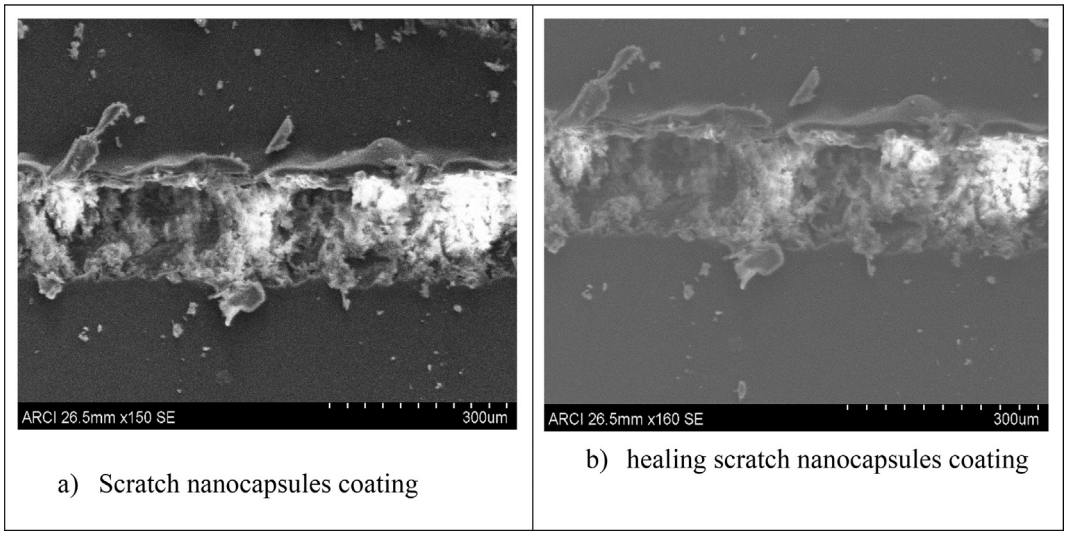

Fig. 14. FESEM image of scratch nanocapsules coating and healing nanocapsules coating.

Figure 11 depicts the Nyquist plot results for coating with and without nanocapsules after 1 day and 14 day contact in 3.5% Salt solution (see Fig. 11). As illustrated in Fig. 12, an appropriate electrical equivalent circuit was chosen to calculate and examine the impedance of coated substrates. The charge transfer resistance (R_2) is parallel to the electrical double layer capacitance (CPE_{edl}), which is in series with the coating resistance in this example (R_{coat}). The Ccoat represents coating capacitance (Cc). Because the experimental data and the model have a high level of agreement. Nyquist plot subsequently 24 h of acquaintance, DBP nanocapsules coated surfaces displayed maximum impedance values in the low-frequency region, representative maximum corrosion inhibition for DBP nanocapsules coated substrates than scratch epoxy coating. As shown in the figure, scratch epoxy coating shows metal oxide-interface and starting corrosion mechanism process, whereas DBP nanocapsules show double layer coating that resists the corrosion process. However, the coating resistance of DBP nanocapsules coating reduced after 14 days of disclosure but still more resistance than scratch epoxy coating (after 24 h exposure, as shown in Fig. 11a). This possibly will have happened to owe to cost of barrier property of coatings since the reduction of coating pore resistance and increase of C_c can be recognized to the diffusion of ions of salt and water into the coating layer. This modification shows corrosion of the coatings barrier in the 3.5% salt solution immersion. The fitting result of Nyquist as shown in Table 2.

3.6. Self-healing study for corrosion inhibition process

The visual change is observed after immersing the coated panel in a salt solution. Monitor this process; keep coating panels in a salt solution for 20 days. Fig. 13 depicts standard coating panels that have been exposed to start the corrosion process, whereas nanocapsules-based coating formulations have not yet rusted. It was exposed that nanocapsules were the primary dynamic mechanism to improve corrosion inhibition. The key reason for nanocapsules covering such corrosion inhibition performance is the release mechanism of dibutyl phthalate from nanocapsules. This dibutyl phthalate produces the swelling polymeric shell by evaporating alcohol from dibutyl phthalate, which forms an external layer on the coating substrate and repairs the damage site while keeping the same mechanical properties as the initial coating (see Fig. 14).

4. Conclusion

This experiment shows that dibutyl phthalate (DBT) can be successfully encapsulated in a polymeric shell (PUF) in the form of nanocapsules using ultrasound. The resulting nanocapsules have a spherical shape and a thick exterior wall thickness of Poly (UF) shell. The particle size distribution is narrow, with an average mean size of 337 nm. Later, prepared nanocapsules with concentrations (2.5, 5, and 10%) encapsulated in epoxy-amine coating formulation provide better corrosion inhibition

performance than without nanocapsules coating, as demonstrated by the Bode and Nyquist plot. As 10% nanocapsules provide better coating resistance than 5 and 2.5% nanocapsules, however, optimum 5% nanocapsules still give the best electrochemical analysis than standard epoxy coating. With a 5% Concentration of nanocapsules-based polymeric shell corrosion inhibition outperformed neat polymeric coatings.

Declaration of competing interest

The authors declare no conflict of interest.

Acknowledgment

The author acknowledges Russian Science Foundation grant 22-26-00079 for supporting this manuscript.

References

[1] B. Bhuvaneshwari, A. Selvaraj, N.R. Iyer, Corrosion inhibitors for increasing the service life of structures, New Mater Civ Eng (2020) 657–676, https://doi.org/10.1016/B978-0-12-818961-0.00020-X.
[2] M.A.J. Mazumder, Global impact of corrosion : occurrence , cost and mitigation, Glob J Eng Sci 5 (2020) 4, https://doi.org/10.33552/GJES.2020.05.000618.
[3] N. Sharma, S. Sharma, S.K. Sharma, R. Mehta, Evaluation of corrosion inhibition and self healing capabilities of nanoclay and tung oil microencapsulated epoxy coatings on rebars in concrete, Construct Build Mater 259 (2020) 120278, https://doi.org/10.1016/j.conbuildmat.2020.120278.
[4] A. Hosseinpour, M. Rezaei Abadchi, M. Mirzaee, F. Ahmadi Tabar, B. Ramezanzadeh, Recent advances and future perspectives for carbon nanostructures reinforced organic coating for anti-corrosion application, Surface Interfac 23 (2021) 100994, https://doi.org/10.1016/j.surfin.2021.100994.
[5] R. Gupta, P. Bhardwaj, D. Mishra, S.K. Sanghi, S.S. Amritphale, Novel non-hydroxyl synthesis and fabrication of advanced hybrid inorganic-organic geopolymeric coating material for corrosion protection, Int J Adhesion Adhes 110 (2021) 102951, https://doi.org/10.1016/j.ijadhadh.2021.102951.
[6] M. Toorani, M. Aliofkhazraei, M. Mahdavian, R. Naderi, Superior corrosion protection and adhesion strength of epoxy coating applied on AZ31 magnesium alloy pre-treated by PEO/Silane with inorganic and organic corrosion inhibitors, Corrosion Sci 178 (2021) 109065, https://doi.org/10.1016/j.corsci.2020.109065.
[7] P.K. Pandis, S. Papaioannou, V. Siaperas, A. Terzopoulos, V. N. Stathopoulos, Evaluation of Zn- and Fe- rich organic coatings for corrosion protection and condensation performance on waste heat recovery surfaces, Int J Thermofluids 3–4 (2020) 100025, https://doi.org/10.1016/j.ijft.2020.100025.
[8] L. Wiering, X. Qi, D. Battocchi, Corrosion performance of high-temperature organic coatings subjected to heat treatments, Prog Org Coatings 159 (2021) 106418, https://doi.org/10.1016/j.porgcoat.2021.106418.
[9] A.A.P. Khan, A. Khan, O. Ansari, M. Shaban, M.A. Rub, N. Azum, et al., Self-healing of polymer materials and their composites, Self-Healing, Compos Mater Des Appl (2020) 103–121, https://doi.org/10.1016/B978-0-12-817354-1.00007-7.
[10] M. Mobaraki, M. Ghaffari, M. Mozafari, Basics of self-healing composite materials, Self-Healing, Compos Mater Des Appl (2019) 15–31.
[11] M. Scheiner, T.J. Dickens, O. Okoli, Progress towards self-healing polymers for composite structural applications, Polymer 83 (2016) 260–282, https://doi.org/10.1016/J.POLYMER.2015.11.008.
[12] A. Yabuki, T. Shiraiwa, I.W. Fathona, pH-controlled self-healing polymer coatings with cellulose nanofibers providing an effective release of corrosion inhibitor, Corrosion Sci 103 (2016) 117–123, https://doi.org/10.1016/j.corsci.2015.11.015.
[13] S. Manasa, A. Jyothirmayi, T. Siva, S. Sathiyanarayanan, K.V. Gobi, R. Subasri, Effect of inhibitor loading into nanocontainer additives of self-healing corrosion protection coatings on aluminum alloy A356.0, J Alloys Compd 726 (2017) 969–977, https://doi.org/10.1016/J.JALLCOM.2017.08.037.
[14] U.D. Bagale, R. Desale, S.H. Sonawane, R.D. Kulkarni, An active corrosion inhibition coating of two pack epoxy polyamide system using halloysite nanocontainer, Protect Met Phys Chem Surface 54 (2018) 230–239, https://doi.org/10.1134/S2070205118020144.
[15] V.V. Gite, P.D. Tatiya, R.J. Marathe, P.P. Mahulikar, D.G. Hundiwale, Microencapsulation of quinoline as a corrosion inhibitor in polyurea microcapsules for application in anticorrosive PU coatings, Prog Org Coating 83 (2015) 11–18, https://doi.org/10.1016/j.porgcoat.2015.01.021.
[16] H. Pulikkalparambil, S. Siengchin, J. Parameswaranpillai, Corrosion protective self-healing epoxy resin coatings based on inhibitor and polymeric healing agents encapsulated in organic and inorganic micro and nanocontainers, Nano Struct Nano Object 16 (2018) 381–395, https://doi.org/10.1016/J.NANOSO.2018.09.010.
[17] X. Cai, D. Fu, A. Qu, Optimization of preparation conditions of epoxy-containing nanocapsules, Sci Eng Compos Mater 24 (2017) 155–161, https://doi.org/10.1515/secm-2014-0469.
[18] D.Y. Zhu, M.Z. Rong, M.Q. Zhang, Self-healing polymeric materials based on microencapsulated healing agents: from design to preparation, Prog Polym Sci 49–50 (2015) 175–220, https://doi.org/10.1016/j.progpolymsci.2015.07.002.
[19] H. Yi, Y. Deng, C. Wang, Pickering emulsion-based fabrication of epoxy and amine microcapsules for dual core self-healing coating, Compos Sci Technol 133 (2016) 51–59, https://doi.org/10.1016/j.compscitech.2016.07.022.
[20] S. An, M.W. Lee, A.L. Yarin, S.S. Yoon, A review on corrosion-protective extrinsic self-healing: comparison of microcapsule-based systems and those based on core-shell vascular networks, Chem Eng J 344 (2018) 206–220, https://doi.org/10.1016/j.cej.2018.03.040.
[21] J.M. Chem, H. Wei, Y. Wang, J. Guo, N.Z. Shen, D. Jiang, et al., Advanced micro/nanocapsules for self-healing smart anticorrosion coatings, JMaterChem A3 (2015) 469–480, https://doi.org/10.1039/c4ta04791e.
[22] E. Shchukina, H. Wang, Nanocontainer-based self-healing coatings: current progress and future perspectives, Chem Commun (2019) 3859–3867, https://doi.org/10.1039/c8cc09982k.
[23] D. Borisova, D. Akçakayiran, M. Schenderlein, H. Möhwald, D.G. Shchukin, Nanocontainer-based anticorrosive coatings: effect of the container size on the self-healing performance, Adv Funct Mater 23 (2013) 3799–3812, https://doi.org/10.1002/adfm.201203715.
[24] R.H. Staff, M. Gallei, K. Landfester, D. Crespy, Hydrophobic nanocontainers for stimulus-selective release in aqueous environments, Macromolecules 47 (2014) 4876–4883, https://doi.org/10.1021/ma501233y.
[25] D.G. Shchukin, Container-based multifunctional self-healing polymer coatings, Polym Chem 4 (2013) 4871, https://doi.org/10.1039/c3py00082f.
[26] M. Wang, M. Liu, J. Fu, An intelligent anticorrosion coating based on pH-responsive smart nanocontainers fabricated via a facile method for protection of carbon steel, J Mater Chem A 3 (2015) 6423–6431, https://doi.org/10.1039/C5TA00417A.
[27] Z. Zheng, M. Schenderlein, X. Huang, N.J. Brownbill, F. Blanc, D. Shchukin, Influence of functionalization of nanocontainers on self-healing anticorrosive coatings, ACS Appl

Mater Interfaces 7 (2015) 22756–22766, https://doi.org/10.1021/acsami.5b08028.
[28] H. Abdipour, M. Rezaei, F. Abbasi, Synthesis and characterization of high durable linseed oil-urea formaldehyde micro/nanocapsules and their self-healing behaviour in epoxy coating, Prog Org Coating 124 (2018) 200–212, https://doi.org/10.1016/J.PORGCOAT.2018.08.019.
[29] S.B. Singh, Nanocapsules: an engineered nanomaterial for smart self-healing coatings and catalysis, Handb Nanomater Manuf Appl (2020) 175–189, https://doi.org/10.1016/B978-0-12-821381-0.00007-7.
[30] J. Sun, Y. Wang, N. Li, L. Tian, Tribological and anticorrosion behavior of self-healing coating containing nanocapsules, Tribol Int 136 (2019) 332–341, https://doi.org/10.1016/J.TRIBOINT.2019.03.062.
[31] Y. Liu, B.M. Budhlall, Self-healing nanocomposites comprised of poly(urea formaldehyde) nanocapsules in a thermosetting polyurea, Eur Polym J 126 (2020) 109545, https://doi.org/10.1016/J.EURPOLYMJ.2020.109545.
[32] M. Akhondi, E. Jamalizadeh, Fabrication of β-cyclodextrin modified halloysite nanocapsules for controlled release of corrosion inhibitors in self-healing epoxy coatings, Prog Org Coating 145 (2020) 105676, https://doi.org/10.1016/J.PORGCOAT.2020.105676.
[33] S. Devadasu, U. Bagale, S.H. Sonawane, S. Suranani, Development of ultra-high build self-healing coatings using amino silanized lignin nanocapsules, Mater, Today Proc 45 (2021) 5745–5751, https://doi.org/10.1016/J.MATPR.2021.02.576.
[34] T. Apolinário de Oliveira, M. D'Orey Gaivão Portela Bragança, I. Miguel Pinkoski, G. Carrera, The effect of silica nanocapsules on self-healing concrete, Construct Build Mater 300 (2021) 124010, https://doi.org/10.1016/J.CONBUILDMAT.2021.124010.
[35] S. Han, S. Lyu, S. Wang, F. Fu, High-intensity ultrasound assisted manufacturing of melamine-urea-formaldehyde/paraffin nanocapsules, Colloid Surf A Physicochem Eng Asp 568 (2019) 75–83, https://doi.org/10.1016/J.COLSURFA.2019.01.054.
[36] M.J. Galindo-Pérez, D. Quintanar-Guerrero, M. de los Á. Cornejo-Villegas, M. de la L. Zambrano-Zaragoza, Optimization of the emulsification-diffusion method using ultrasound to prepare nanocapsules of different food-core oils, Lebensm Wiss Technol 87 (2018) 333–341, https://doi.org/10.1016/J.LWT.2017.09.008.
[37] S.P. Carneiro, R.M. Cruz, O.D.H. Dos Santos, Evaluation of short cycles of ultrasound application in nanoemulsions to obtain nanocapsules, Ultrason Sonochem 27 (2015) 536–542, https://doi.org/10.1016/J.ULTSONCH.2015.04.002.
[38] U.D. Bagale, S.H. Sonawane, B.A. Bhanvase, R.D. Kulkarni, R. Gogate, Green synthesis of nanocapsules for self-healing anticorrosion coating using ultrasound-assisted approach, 2018, pp. 147–159, https://doi.org/10.1515/gps-2016-0160.
[39] A.C. Jackson, J.A. Bartelt, P.V. Braun, Transparent self-healing polymers based on encapsulated plasticizers in a thermoplastic matrix, Adv Funct Mater 21 (2011) 4705–4711, https://doi.org/10.1002/adfm.201101574.
[40] Y. Cao, H. Wu, S.I. Allec, B.M. Wong, D.S. Nguyen, C. Wang, A highly stretchy, transparent elastomer with the capability to automatically self-heal underwater, Adv Mater 30 (2018), https://doi.org/10.1002/adma.201804602.
[41] I. Radovic, A. Stajcic, A. Radisavljevic, F. Veljkovic, M. Cebela, V.V. Mitic, et al., Solvent effects on structural changes in self-healing epoxy composites, Mater Chem Phys 256 (2020) 123761, https://doi.org/10.1016/J.MATCHEMPHYS.2020.123761.
[42] T. Thakur, B. Gaur, A.S. Singha, Bio-based epoxy/imidoamine encapsulated microcapsules and their application for high performance self-healing coatings, Prog Org Coating 159 (2021) 106436, https://doi.org/10.1016/J.PORGCOAT.2021.106436.
[43] S. Gao, X. Dong, J. Huang, J. Dong, Y. Cheng, Z. Chen, et al., Co-solvent induced self-roughness superhydrophobic coatings with self-healing property for versatile oil-water separation, Appl Surf Sci 459 (2018) 512–519, https://doi.org/10.1016/J.APSUSC.2018.08.041.
[44] A.G. Cordeiro Neto, A.C. Pellanda, A.R. de Carvalho Jorge, J. B. Floriano, M.A. Coelho Berton, Preparation and evaluation of corrosion resistance of a self-healing alkyd coating based on microcapsules containing Tung oil, Prog Org Coating 147 (2020) 105874, https://doi.org/10.1016/j.porgcoat.2020.105874.
[45] M. Behzadnasab, S.M. Mirabedini, M. Esfandeh, R.R. Farnood, Evaluation of corrosion performance of a self-healing epoxy-based coating containing linseed oil-filled microcapsules via electrochemical impedance spectroscopy, Prog Org Coating 105 (2017) 212–224, https://doi.org/10.1016/j.porgcoat.2017.01.006.
[46] J. Li, H. Shi, F. Liu, E.H. Han, Self-healing epoxy coating based on tung oil-containing microcapsules for corrosion protection, Prog Org Coatings 156 (2021) 106236, https://doi.org/10.1016/j.porgcoat.2021.106236.
[47] M. Samadzadeh, S.H. Boura, M. Peikari, A. Ashrafi, M. Kasiriha, Tung oil: an autonomous repairing agent for self-healing epoxy coatings, Prog Org Coating 70 (2011) 383–387, https://doi.org/10.1016/j.porgcoat.2010.08.017.